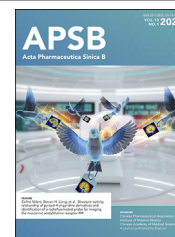




Chinese Pharmaceutical Association
Institute of Materia Medica, Chinese Academy of Medical Sciences

Acta Pharmaceutica Sinica B

www.elsevier.com/locate/apsb
www.sciencedirect.com



ORIGINAL ARTICLE

Reactivation of PPAR α alleviates myocardial lipid accumulation and cardiac dysfunction by improving fatty acid β -oxidation in *Dsg2*-deficient arrhythmogenic cardiomyopathy

Yubi Lin^{b,†}, Ruonan Liu^{a,†}, Yanling Huang^a, Zhe Yang^c,
Jianzhong Xian^c, Jingmin Huang^a, Zirui Qiu^a, Xiufang Lin^c,
Mengzhen Zhang^d, Hui Chen^e, Huadong Wang^f, Jiana Huang^g,
Geyang Xu^{a,*}

^aDepartment of Physiology, School of Medicine, Jinan University, Guangzhou 510632, China

^bThe First Dongguan Affiliated Hospital, Guangdong Medical University, Dongguan 523710, China

^cThe Cardiovascular Center, Department of Cardiology, Interventional Medical Center, Guangdong Provincial Key Laboratory of Biomedical Imaging and Guangdong Provincial Engineering Research Center of Molecular Imaging, the Fifth Affiliated Hospital, Sun Yat-sen University, Zhuhai 519000, China

^dGuangdong Provincial Cardiovascular Institute, Guangdong Provincial People's Hospital, Guangzhou 510080, China

^eBiotherapy Center; Cell-gene Therapy Translational Medicine Research Center, the Third Affiliated Hospital, Sun Yat-sen University, Guangzhou 510630, China

^fDepartment of Pathophysiology, School of Medicine, Jinan University, Guangzhou 510632, China

^gReproductive Medicine Center, the Six Affiliated Hospital, Sun Yat-sen University, Guangzhou 51000, China

Received 6 January 2022; received in revised form 27 March 2022; accepted 2 April 2022

KEY WORDS

Arrhythmogenic
cardiomyopathy;
Desmosome;
Desmoglein2;

Abstract Arrhythmogenic cardiomyopathy (ACM), a fatal heart disease characterized by fibroadipocytic replacement of cardiac myocytes, accounts for 20% of sudden cardiac death and lacks effective treatment. It is often caused by mutations in desmosome proteins, with Desmoglein-2 (DSG2) mutations as a common etiology. However, the mechanism underlying the accumulation of fibrofatty in ACM remains unknown, which impedes the development of curative treatment. Here we investigated the fat

*Corresponding author. Tel.: +86 20 85220260; fax: +86 20 85221343.

E-mail address: xugeyangliang@163.com (Geyang Xu).

[†]These authors made equal contributions to this work.

Peer review under responsibility of Chinese Pharmaceutical Association and Institute of Materia Medica, Chinese Academy of Medical Sciences.

<https://doi.org/10.1016/j.apsb.2022.05.018>

2211-3835 © 2023 Chinese Pharmaceutical Association and Institute of Materia Medica, Chinese Academy of Medical Sciences. Production and hosting by Elsevier B.V. This is an open access article under the CC BY-NC-ND license (<http://creativecommons.org/licenses/by-nc-nd/4.0/>).



Heart failure;
Lipid accumulation;
mTOR;
PPAR α ;
FA oxidation

accumulation and the underlying mechanism in a mouse model of ACM induced by cardiac-specific knockout of *Dsg2* (CS-*Dsg2*^{-/-}). Heart failure and cardiac lipid accumulation were observed in CS-*Dsg2*^{-/-} mice. We demonstrated that these phenotypes were caused by decline of fatty acid (FA) β -oxidation resulted from impaired mammalian target of rapamycin (mTOR) signaling. Rapamycin worsened while overexpression of mTOR and 4EBP1 rescued the FA β -oxidation pathway in CS-*Dsg2*^{-/-} mice. Reactivation of PPAR α by fenofibrate or AAV9-*Ppara* significantly alleviated the lipid accumulation and restored cardiac function. Our results suggest that impaired mTOR–4EBP1–PPAR α -dependent FA β -oxidation contributes to myocardial lipid accumulation in ACM and PPAR α may be a potential target for curative treatment of ACM.

© 2023 Chinese Pharmaceutical Association and Institute of Materia Medica, Chinese Academy of Medical Sciences. Production and hosting by Elsevier B.V. This is an open access article under the CC BY-NC-ND license (<http://creativecommons.org/licenses/by-nc-nd/4.0/>).

1. Introduction

Arrhythmogenic cardiomyopathy (ACM) is a heritable cardiac disease associated with ventricular arrhythmias, heart failure (HF), thromboembolism and sudden cardiac death (SCD) especially in young athletes¹. It is believed to be responsible for up to 20% of SCD cases². Up to now, there is no effective treatment for ACM, while the main goal of treatment is the prevention of SCD³. ACM is pathologically characterized by a progressive loss of cardiomyocytes and fibro-fatty tissue replacement predominantly in the right ventricle (RV), with left ventricular (LV) or bilateral ventricular involvement in some cases^{1,4}. More than 50% ACM patients present one or more mutations in genes encoding structural proteins especially those consist the cardiac desmosomes, including desmoglein2 (DSG2)⁵, desmocollin2⁶, plakoglobin⁷, desmoplakin⁸ and plakophilin-2⁹. Desmosomes are specialized and highly ordered membrane structures that mediate cell–cell contact and strong adhesion. Desmosomes contribute to the mechanical integrity of the myocardium by anchoring the intermediate filament system to the plasma membrane in adjacent cells^{10,11}. DSG2 is a major cadherin of the cardiac desmosome and connect neighboring cardiomyocytes with desmocollin2 *via* interaction of their extracellular domains^{12,13}. *Dsg2* mutations are the second common etiology of ACM and associate with worst prognosis¹⁴. Transgenic mice overexpressing the mutation of *Dsg2* *p.N271S* exhibit a progressive cardiomyocyte loss and fibroadipocytic replacement, which is associated with severe heart muscle diseases such as ACM¹⁵. In another study, mice carrying a deletion of the adhesive extracellular domain of *Dsg2* also developed ARVC-like phenotype with fibrotic lesion and lipid droplet detected in the heart more frequently than in wild-type mice¹⁶.

Impaired energy supply is regarded as the major cause of cardiac dysfunction in ACM patients¹⁷. The cardiac excitation–contraction coupling consumes the majority of the ATP produced by the mitochondria to fuel incessant activity¹⁸. Under normal conditions, 60%–90% of the ATP supply in heart relies on fatty acid (FA) oxidation, while the remaining 10%–40% is derived from pyruvate oxidation¹⁹. However, in pathological scenarios, development of overt cardiac dysfunction is accompanied by decline in FA oxidation rates, which has been confirmed in different species and models of HF, including ischaemic²⁰ and pacing-induced²¹ HF, as well as in humans end-stage HF^{22,23}. The decrease in FA oxidation might be explained at least in part by the suppression of peroxisome proliferator-activated receptors α (PPAR α) signaling²⁴. PPAR α is a nuclear receptor with most

abundant expression in the myocardium, where it upregulates the transcription of genes related to FA uptake and oxidation with PPAR γ co-activator 1 α (PGC1 α)²⁵.

Mechanistic target of rapamycin (mTOR), served as an intracellular fuel sensor, is vital for the maintenance of cardiac structure and function in the postnatal period and adulthood^{26,27}. Cardiac-specific mTOR-knockout embryos present a significant reduction in cardiomyocyte proliferation and an increase in apoptosis, which results in cardiac dilation and dysfunction, with signs of terminal HF²⁸. Overexpression of eukaryotic initiation factor 4E (eIF4E) binding protein (4E-BP), one of mTORC1 downstream target, leads to enhanced mitochondrial respiration with increased PGC-1 α translation²⁹. Activation of PGC1 α /PPAR α /mTOR pathway plays a significant role in maintaining the oxidative metabolism/glycolysis balance and improves mitochondrial function in rat models of HF³⁰. These findings inspired the hypothesis that mTOR–4EBP1–PPAR α pathway plays a role in ACM-related cardiac dysfunction and lipid accumulation. To test this hypothesis, we examined this pathway and its involvement in FA oxidation and cardiac function in an ACM mouse model induced by cardiac-specific *Dsg2* knockout. We show that mTOR–4EBP1–PPAR α axis in cardiac muscle is essential for the energy supply by FA oxidation and normal heart function. Furthermore, reactivation of PPAR α by fenofibrate (a PPAR α agonist) or cardiac-specific overexpression of PPAR α rescues the impaired cardiac morphology and function resulted from cardiac *Dsg2* deletion, suggesting PPAR α is a potential target for ACM treatment.

2. Materials and methods

2.1. Materials

Rapamycin, DMSO and fenofibrate were purchased from Sigma–Aldrich (St. Louis, MO, USA). Rabbit anti-phospho-mTOR (Ser2448), anti-mTOR, anti-phospho-4EBP1 (Thr37/46), anti-4EBP1, anti-PGC1 α antibodies and mouse monoclonal anti- β -actin were from Cell Signaling Technology (Beverly, MA, USA). Rabbit anti-DSG2, anti-PPAR α , anti-CPT1b, anti-ACADL, anti-GAPDH antibodies were from Abcam Inc. (Cambridge, MA, USA). Horseradish peroxidase-conjugated, donkey anti-rabbit IgG and donkey anti-mouse IgG were from Jackson ImmunoResearch (West Grove, PA, USA). Immobilon western chemiluminescent HRP substrate was purchased from Millipore (Temecula, CA, USA). Trizol reagent and the reverse transcription (RT) system were purchased from Promega Inc. (Madison, WI, USA).

2.2. Animals and treatments

Cardiac-specific *Dsg2* knockout mice (CS-*Dsg2*^{-/-}) were generated using a standard strategy of Cre-LoxP recombination. The targeting vector contained 1.9 kb 5'-homologous arm, flox region, PGK-NeopolyA marker, 3.3 kb 3'-homologous arm and MC1-TK-polyA negative selection marker. An FRT-flanked Neo cassette was inserted to 3'-homologous arm, and two LoxP sites were introduced to 5'-homologous arm and 3' of Neo, respectively. Chimeric mice carrying the Neo-floxed *Dsg2* allele were crossed with Flp mice (C57BL/6J background) to remove the Neo cassette to obtain F1 mice (*Dsg2*^{fl-neo/+}). Alternatively, *Dsg2*^{fl-neo/+} mice were crossed with Ckmm-Cre mice (C57BL/6J background) to obtain *Dsg2*^{+/+} (wild-type; WT), *Dsg2*^{+/-} (heterozygous; HET) and *Dsg2*^{-/-} (homozygote; -/-) mice. Animals used in this study were handled in accordance with the Guide for the Care and Use of Laboratory Animals published by the National Institutes of Health (NIH Publications No. 8023, revised 1978). All animal protocols were approved by the Animal Care and Use Committee of Jinan University (Guangzhou, China).

8–14-week mice were kept on a regular chow diet (Research Diets Inc., 10% fat) and allowed *ad libitum* access to food and water.

To verify the effect of mTOR signaling on myocardial lipid metabolism after *Dsg2* knockout, 8–10-week-old WT and CS-*Dsg2*^{-/-} mice were tail vein injected with dimethyl sulfoxide (DMSO) or rapamycin (1 mg/kg) for 9 consecutive days.

To determine whether PPAR α reactivation ameliorate heart lipid metabolism and function after *Dsg2* knockout, the PPAR α agonist fenofibrate (Sigma–Aldrich, dissolved in 0.75% [w/v] cellulose carrier solution) was administered by daily oral gavage at a dose of 150 mg per kg body weight for 4 weeks; CS-*Dsg2*^{-/-} mice were tail vein injected with adeno-associated virus containing green fluorescent protein (AAV9-cTnT-GFP, 5×10^{11} vg per mouse) or adeno-associated virus containing peroxisome proliferator-activated receptors α (AAV9-cTnT-*Ppara*, 5×10^{11} vg per mouse) 28 days before sacrifice.

2.3. AAV9-cTnT promoter-*Ppara* construction

To construct the plasmid for cardiomyocyte-specific *Ppara* over-expression, coding sequence of mouse *Ppara* was inserted into AAV-cTnT-promoter vector. Then the recombinant plasmid and its control plasmid (AAV-cTnT promoter) were transfected into 293T cells for virus packaging. Virus was purified and concentrated by gradient centrifugation. AAV9 titer was determined by quantitative PCR.

2.4. Transthoracic echocardiography

Echocardiographic measurements were performed on mice, anesthetized with 1%–2% isoflurane gas, using the Vevo2100 High Resolution *In Vivo* Imaging System (Visual Sonics, Toronto, Canada) with a SL3116 high-frequency linear array probe and a 22 MHz transducer. HR (heart rate), the thickness of left ventricular anterior wall in diastole period (LVAW;d) and in systole period (LVAW;s), the thickness of left ventricular posterior wall in diastole period (LVPW;d) and in systole period (LVPW;s), ejection fraction of left ventricle (EF), the short axis shortening rate of left ventricle (FS), cardiac output per minute of left ventricle (CO), stroke volume of left ventricle (SV), the diameter of left ventricle in systole period (Diameter;s) and in diastole period (Diameter;d), the volume of left ventricle in systole period (V;s) and in diastole period (V;d) were measured digitally on M-mode tracing.

2.5. Histological analysis

Heart samples were harvested, fixed in 4% paraformaldehyde, paraffin-embedded, cut into 3- μ m sections and stained with hematoxylin–eosin (H&E) according to standard procedures. For Oil red O staining, frozen sections (6 μ m) of heart were stained in 0.5% Oil red O solution for 2 h in a 50 °C oven and then in 85% propylene glycol solution for 5 min. Sections were rinsed in distilled water, stained in Gill's hematoxylin for 2 s, washed, and mounted with aqueous mounting medium.

2.6. Determine of triglyceride and free fatty acid in heart and plasma

The triglyceride and free fatty acid content in heart tissue and plasma were measured according to the manufacturer's instructions (Boxbio, Beijing, China). Values were normalized to protein concentration. For human plasma triglyceride measurement, ACM patients and normal participants were recruited in current study. Participation in this study was voluntary and written informed consent was obtained from each participant. The guidelines of the Declaration of Helsinki of the World Medical Association were followed. All protocols were approved by the Guangdong Medical Institutional Review Board and Medical Ethics Committees [No. GDREC2016001H(R1)].

2.7. Fatty acid β -oxidation rate analysis and quantification of cardiac ATP

Myocardial mitochondria were isolated integrally by Mitochondrial Isolation Kit (Beyotime, Jiangsu, China). Then the mitochondria were used to investigate fatty acid β -oxidation rate according to the Fatty Acid β -oxidation Kit from Genmed Scientifics Inc., USA.

ATP contents were measured in the heart tissues (20 mg) of mice after overnight fasting by using the ATP Colorimetric/Fluorometric Assay Kit (BioVision).

2.8. Cell culture and treatment

The murine atrial cardiac myocyte cell line HL-1 was purchased from Sigma–Aldrich and maintained at 37 °C in an atmosphere of 5% CO₂. For transient transfection, cells were plated at optimal densities and grown for 24 h. Cells were then transfected with *Dsg2* siRNA using lipofectamine reagent according to the manufacturer's instructions. Twenty-four hours after transfection, the cells were treated with DMSO or fenofibrate (100 μ mol/L) for another 24 h, or treated with *Gfp* or AAV9-*Ppara* (AAV9-cTnT-*Ppara*, 1.5×10^{11} vg/mL) for 48 h. To investigate the effect of mTOR signaling on FA oxidation after *Dsg2* knockdown, *mTOR* or *4Ebp1* plasmid was co-transfected with *Dsg2* siRNA for 48 h.

2.9. Quantitative real-time PCR

Quantitative real-time PCR was performed as described previously³¹. Primers used in this study were shown in [Supporting Information Table S1](#). For gene expression analysis, RNA was isolated from mouse tissues using TRIzol and reverse-transcribed into cDNAs using the First-Strand Synthesis System for RT-PCR kit. SYBR Green-based real-time PCR was performed using the Mx3000 multiplex quantitative PCR system (Stratagene, La Jolla, CA, USA).

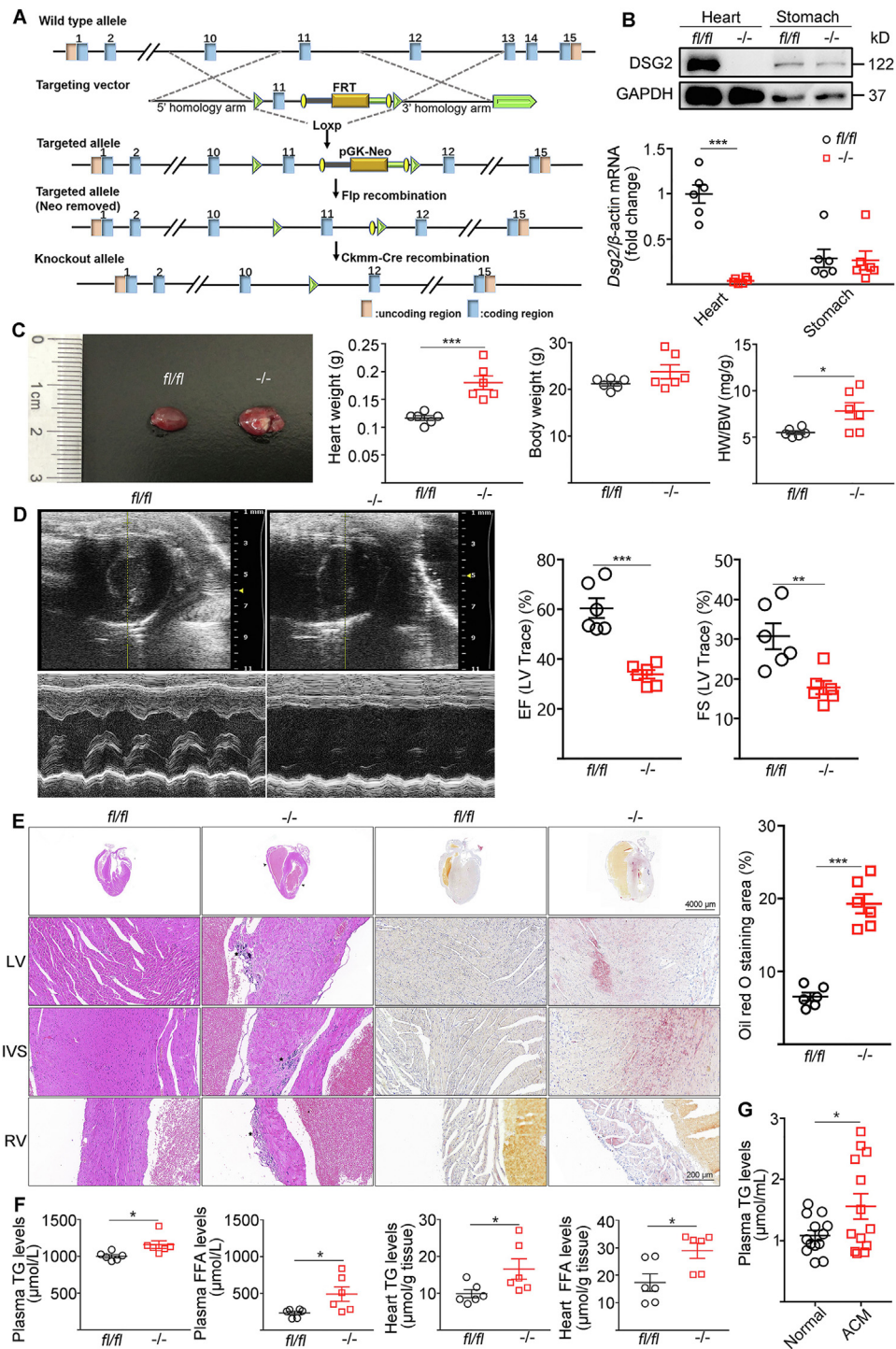


Figure 1 Cardiac-specific *Dsg2* deletion provoked cardiac dysfunction and lipid accumulation. (A) Strategy used for generating CS-*Dsg2*^{-/-} mice. (B) mRNA and protein levels of DSG2 were assessed in the heart and stomach of WT (*fl/fl*) and CS-*Dsg2*^{-/-} (-/-) mice. (C) Representative heart image, heart weight, body weight and heart/body weight ratio. (D) Representative echocardiographic images (M-Mode). Ejection fraction (EF) and Left ventricular fractional shortening (FS) were calculated from the echocardiographic tracings as previously described. (E) HE staining and Oil red O staining of heart sections. Arrow shows dilated atrium, thinning atrial and ventricular wall, asterisk shows myocardial calcification, fibrosis and atrophy. (F) Plasma triglyceride, plasma free fatty acid, heart triglyceride and free fatty acid levels of WT and CS-*Dsg2*^{-/-} mice ($n = 6$, results are expressed as mean values \pm SEM. * $P < 0.05$, ** $P < 0.01$, *** $P < 0.001$ vs. WT mice). (G) Plasma triglyceride levels of normal and ACM patients ($n = 13$, results are expressed as mean values \pm SEM. * $P < 0.05$ vs. normal subjects).

2.10. Western blot analysis

Protein extracts were electrophoresed, blotted, and then incubated with primary antibodies. The antibodies were detected using 1:10,000 horseradish peroxidase-conjugated, donkey anti-rabbit IgG and donkey anti-mouse IgG (Jackson ImmunoResearch, USA). A Western blotting luminol reagent was used to visualize bands corresponding to each antibody. The band intensities were quantitated by Image J software.

2.11. Statistical analysis

All data are expressed as mean values \pm standard error of mean (SEM). Statistical differences were evaluated by one-way ANOVA followed by Newman-Student-Keuls test or Student's *t*-test. Differences were considered statistically significant with *P* values < 0.05 .

3. Results

3.1. Cardiac-specific *Dsg2* null provokes cardiac dysfunction and lipid accumulation

We first generated an ACM mouse model by crossing *Dsg2*^{fl-neo/+} mice with *Ckmm-Cre* mice which resulted in cardiac-specific *Dsg2* deletion (*CS-Dsg2*^{-/-}) (Fig. 1A). Loss of *Dsg2* was confirmed in the heart by Western blot but not observed in the stomach of *CS-Dsg2*^{-/-} mice (Fig. 1B). Cardiac specific *Dsg2* deletion cause 13.9% sudden

death rate within 3 weeks after birth (Supporting Information Fig. S1). At 12 weeks of age, *CS-Dsg2*^{-/-} mice showed increased in heart weight by 1.5-fold compared to control mice (*Dsg2*^{fl/fl}) (0.18 ± 0.01 g for *CS-Dsg2*^{-/-} mice versus 0.12 ± 0.01 g for controls, *P* = 0.0007, *n* = 6) (Fig. 1C). Ventricular tachycardia, atrio-ventricular block and right bundle branch block were recorded in *CS-Dsg2*^{-/-} mice (Supporting Information Fig. S2). Dilatation of the right ventricle (RV) and impaired contractile function were observed in 12-week-old *CS-Dsg2*^{-/-} mice by transthoracic echocardiography (Fig. 1D, Supporting Information Table S2). H&E staining and Oil red O staining also indicated structural disorders and accumulation of lipid in cardiomyocytes after *Dsg2* gene deletion (Fig. 1E). No abnormality was observed in other tissues such as brown adipose tissue (BAT), white adipose tissue (WAT), liver, skeletal muscle, pancreas and ileum (Supporting Information Fig. S3). Consistent to the results of Oil red O staining, cardiac specific *Dsg2* gene deletion significantly increased plasma and heart triglyceride (TG) levels (Fig. 1F). Similarly, higher TG level was observed in 13 ACM patients than normal controls (Fig. 1G). These results suggest that cardiac-specific *Dsg2* deletion was sufficient to provoke cardiac dysfunction and myocardial lipid accumulation.

3.2. Impaired FA β -oxidation in *CS-Dsg2*^{-/-} mice

The systolic dysfunction of heart is closely related to myocardial energy supply. A healthy heart relies predominantly (60%–90%) on FA oxidation for ATP production¹⁹. Therefore, we next investigated

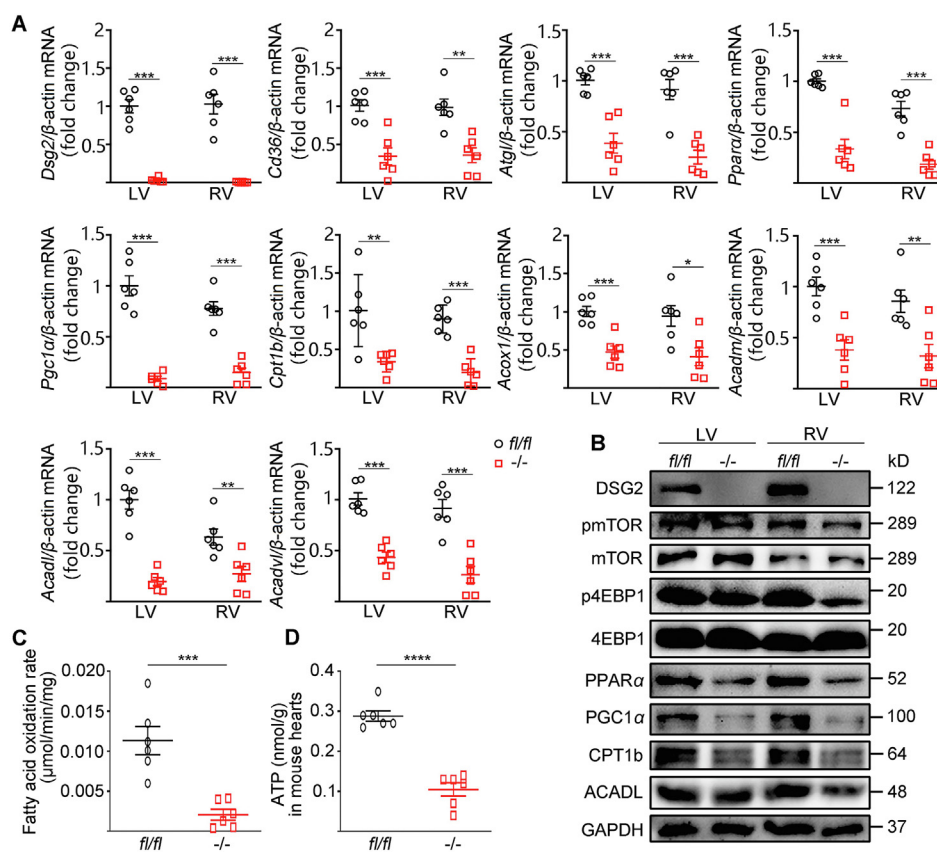


Figure 2 Decreased FA β -oxidation and mTOR–4EBP1 signaling in *CS-Dsg2*^{-/-} mice. (A) Results of quantitative PCR analysis of *Dsg2*, *Cd36*, *Atgl*, *Ppara*, *Pgc1a*, *Cpt1b*, *Acox1*, *Acadm*, *Acadl* and *Acadvl* mRNA levels in LV and RV are expressed as fold change of control using β -actin as loading control. (B) Representative Western blots from WT and *CS-Dsg2*^{-/-} mice. DSG2, pmTOR, p4EBP1, PPAR α , PGC1 α , CPT1b and ACADL were detected using specific antibodies. mTOR, 4EBP1 and GAPDH were used as loading controls. Cardiac fatty acid oxidation rate (C) and ATP content (D) of WT and *CS-Dsg2*^{-/-} mice. Results are expressed as mean values \pm SEM. *n* = 6. **P* < 0.05, ***P* < 0.01, ****P* < 0.001 vs. WT mice.

the FA oxidation pathway in heart in CS-*Dsg2*^{-/-} mice. Downregulation of transcription factors PPAR α and PGC1 α , as well as enzymes involved in FA oxidation, including carnitine palmitoyl-transferase 1b (CPT1b), acyl-CoA oxidase (*Acox1*), medium-chain acyl-CoA dehydrogenase (ACADM), long-chain acyl-CoA dehydrogenase (ACADL), very long-chain acyl-CoA dehydrogenase (ACADVL) were observed in both LV and RV of CS-*Dsg2*^{-/-} mice compared to control mice (Fig. 2A and B). We further measured the fatty acid β -oxidation rate of the heart. As shown in Fig. 2C and D, the fatty acid β -oxidation rate and ATP concentration was significantly lower in the heart of CS-*Dsg2*^{-/-} than controls.

3.3. Downregulation of mTOR–4EBP impairs FA oxidation and cardiac function in CS-*Dsg2*^{-/-} mice

mTOR–4EBP pathway is essential for the maintenance of cardiac structure and function in the postnatal period and adulthood^{26,27,32}. In our study, decreased phosphorylation of mTOR (Ser2448) and 4EBP1 (Thr37/46) were observed in both LV and RV of CS-*Dsg2*^{-/-} mice (Fig. 2B and Supporting Information Fig. S4A).

Rapamycin, a well-documented mTORC1 inhibitor, further exacerbated cardiac hypertrophy and lipid accumulation in CS-*Dsg2*^{-/-} mice (Fig. 3A–C). Rapamycin led to decreased phosphorylation of mTOR and 4EBP1 and suppressions of PPAR α and PGC1 α , as well as their target genes *Cpt1b*, *Acox1*, *Acadm*, *Acadl* and *Acadvl* in the heart (especially the RV) of CS-*Dsg2*^{-/-} mice (Fig. 3D, E and Fig. S4B).

We further investigated whether loss of *Dsg2* directly affected mTOR and FA β -oxidation in a cardiac myocyte cell line HL-1. Consistent to the *in vivo* study, *Dsg2* siRNA knockdown of *Dsg2* led to downregulation of mTOR–4EBP1 and β -oxidation pathway (Supporting Information Fig. S5A, S5B and Fig. S6A), while overexpression of both *mTOR* and *4EBP1* reversed the decline of β -oxidation in HL-1 cells (Fig. S5C, S5D and Fig. S6B).

3.4. PPAR α activation alleviates cardiac dysfunction and lipid accumulation in CS-*Dsg2*^{-/-} mice

Next, we assessed whether lipid accumulation and cardiac function can be improved by treating CS-*Dsg2*^{-/-} mice with

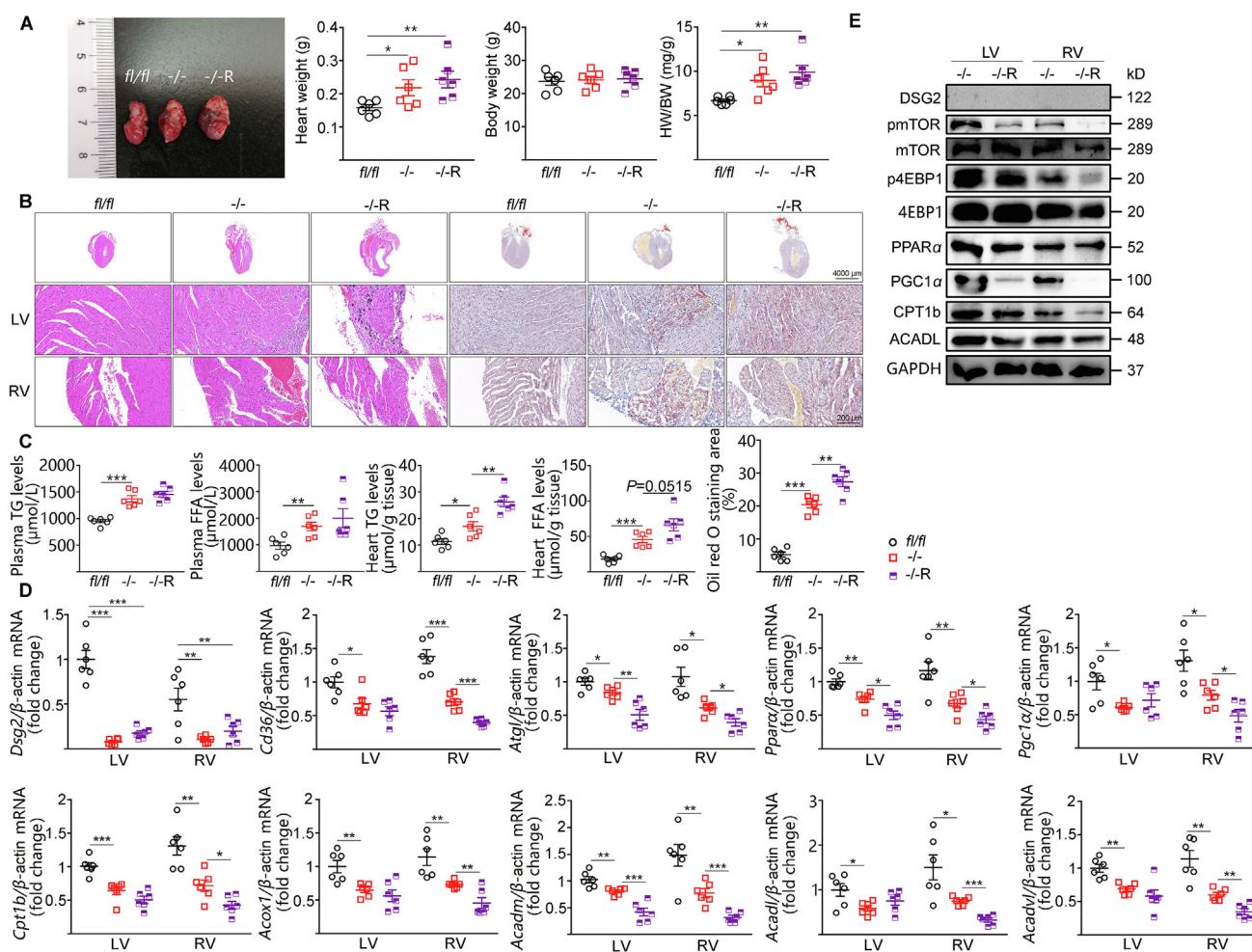


Figure 3 Rapamycin exacerbated cardiac function and hypertrophy in CS-*Dsg2*^{-/-} mice. (A) Representative heart image, heart weight, body weight and heart/body weight ratio of WT, CS-*Dsg2*^{-/-} and CS-*Dsg2*^{-/-} mice received rapamycin (-/-R, 1 mg/kg body weight, tail vein injection). (B) HE staining and Oil red O staining of heart sections. (C) Triglyceride and free fatty acid levels in plasma and heart. (D) Results of quantitative PCR analysis for *Dsg2*, *Cd36*, *Atgl*, *Ppar α* , *Pgc1 α* , *Cpt1b*, *Acox1*, *Acadm*, *Acadl* and *Acadvl* mRNA levels in mouse heart are expressed as fold change of control using β -actin as loading control. (E) Representative Western blots for DSG2, pmTOR, mTOR, p4EBP1, 4EBP1, PPAR α , PGC1 α , CPT1b, ACADL and GAPDH. Results are expressed as mean values \pm SEM. $n = 6$. * $P < 0.05$, ** $P < 0.01$, *** $P < 0.001$.

fenofibrate, a PPAR α agonist treating dyslipidemia widely in clinic. Fenofibrate (150 mg/kg/day, for 4 weeks) decreased the size and weight of heart (Fig. 4A). Meanwhile, improved heart function was shown in CS-*Dsg2*^{-/-} mice after fenofibrate treatment (Fig. 4B, Supporting Information Table S3). Fenofibrate also significantly reversed structural disorders and myocardial accumulation of lipid in CS-*Dsg2*^{-/-} mice (Fig. 4C and D).

Improvement of cardiac function and morphology by fenofibrate was associated with increased FA β -oxidation (Fig. 5, and Fig. S4C). Furthermore, fenofibrate also reversed lipid accumulation and reactivated FA β -oxidation in *Dsg2* knockdown HL-1 cells (Supporting Information Fig. S7A–S7C and S6C).

Finally, we examined whether cardiac-specific reactivation of PPAR α could relief lipid accumulation and restore cardiac function in *Dsg2*^{-/-} mice. Tail vein injection of AAV9-cTnT promoter-*Ppara* into CS-*Dsg2*^{-/-} mice significantly decreased

the size and weight of heart (Fig. 6A and B). Ameliorative LV systolic function and reduced myocardial lipid accumulation were observed in CS-*Dsg2*^{-/-} mice after administration of AAV9-*Ppara* (Fig. 6C–E, Supporting Information Table S4). Moreover, most of FA β -oxidation related genes expression and the fatty acid β -oxidation rate were restored after *Ppara* over-expression (Fig. 6F–I). Consistent with the *in vivo* results, increased mRNA and protein level associated with FA β -oxidation was observed upon PPAR α activation in *Dsg2* siRNA-treated HL-1 cells (Supporting Information Fig. S8A, S8B and Fig. S6D).

4. Discussion

First systematically described in 1980s, ACM is demonstrated to be a common cause of SCD among young adults^{33,34}. Mutations in

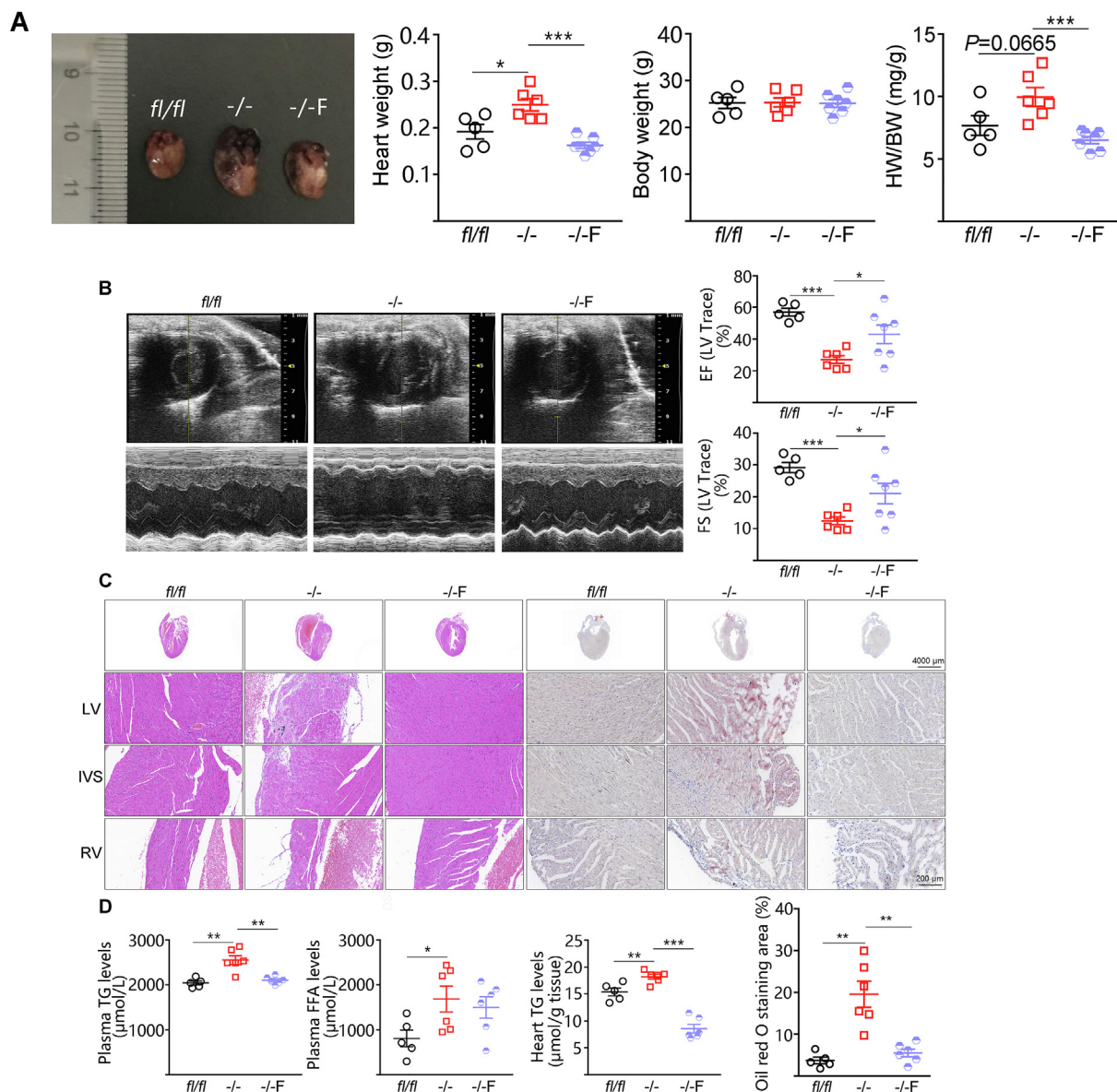


Figure 4 Fenofibrate improved cardiac dysfunction and lipid accumulation in CS-*Dsg2*^{-/-} mice. (A) Representative heart image, heart weight, body weight and heart/body weight ratio of WT, CS-*Dsg2*^{-/-} and CS-*Dsg2*^{-/-} mice received fenofibrate (-/-F). (B) Representative echocardiographic images (M-Mode), EF and FS. (C) H&E staining and Oil red O staining of heart sections. (D) Plasma triglyceride, plasma free fatty acid, and heart triglyceride levels. Results are expressed as mean values \pm SEM. $n = 5-7$. * $P < 0.05$, ** $P < 0.01$, *** $P < 0.001$.

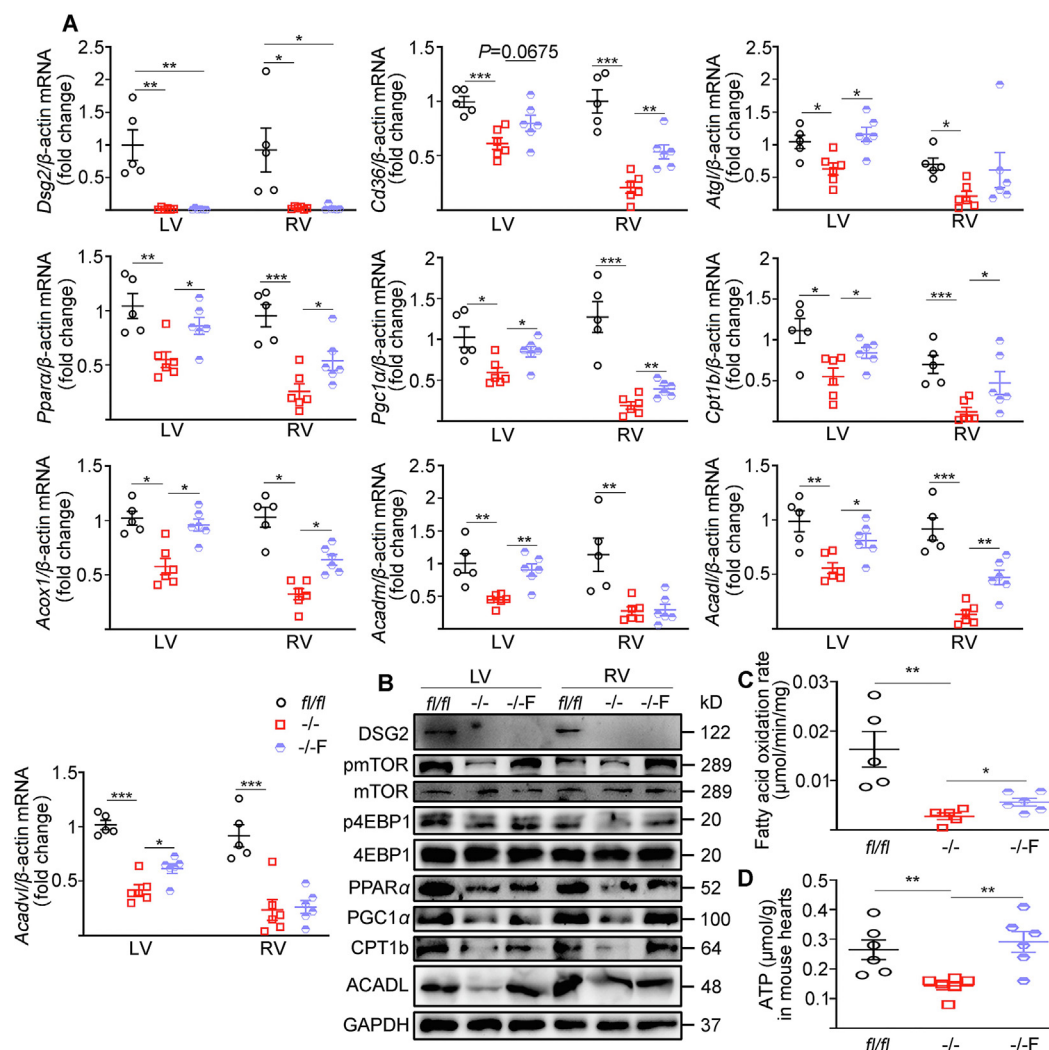


Figure 5 Fenofibrate rescued the declined FA β -oxidation relative pathway in CS-*Dsg2*^{-/-} mice. (A) Results of quantitative PCR analysis for *Dsg2*, *Cd36*, *Atgl*, *Ppar α* , *Pgc1 α* , *Cpt1b*, *Acox1*, *Acadm*, *Acadl* and *Acadvl* mRNA levels are expressed as fold change of control using β -actin as loading control. (B) Representative Western blots of DSG2, pmTOR, mTOR, p4EBP1, 4EBP1, PPAR α , PGC1 α , CPT1b, ACADL and GAPDH. Fatty acid oxidation rate (C) and ATP content (D) of heart. Results are expressed as mean values \pm SEM. $n = 5-7$. * $P < 0.05$, ** $P < 0.01$, *** $P < 0.001$.

desmosomal genes account for $\sim 50\%$ ACM patients in different cohorts, among which *DSG2* mutation is a common type³⁵. *DSG2* mutation can induce many clinical cardiomyopathy phenotypes, including ACM, dilated cardiomyopathy and left ventricular noncompaction, while ACM is most fatal and prone to cause HF and SCD in young adults^{36,37}. Global *Dsg2* knockout is embryonically lethal in mice³⁸. In our present study, we generated an ACM mouse model by cardiac-specific *Dsg2* knockout using Cre-loxp system. As it is expected, cardiac fibrosis and lipid accumulation, as well as impaired contractile function were observed in CS-*Dsg2*^{-/-} which recapitulated the ACM phenotypes in human.

Although it is clear that mutations of desmosome proteins can cause ACM, the mechanism underlying the fatty deposition remain elusive. The cardiac excitation-contraction coupling consumes the majority of ATP to fuel the incessant activity. To sustain sufficient ATP generation, the heart acts as an “omnivore” and can use a variety of different carbon substrates as energy sources if

available, among which the FA β -oxidation provides 60%–90% of total ATP consumption¹⁸. In our study, we observed down-regulation of adipose triglyceride lipase (*Atgl*), FA transport protein CD36, CPT1b, and FA oxidation enzymes *Acox1*, *ACADM*, *ACADL*, *ACADVL* in CS-*Dsg2*^{-/-} mice. The cardiac FA β -oxidation rate was significantly impaired after *Dsg2* deletion. This is consistent to a recent finding that ACM patients have a different metabolome compared to healthy controls, and mainly affected beta oxidation of fatty acids¹⁷. It is also regarded that lipid accumulation in the heart is associated with arrhythmogenicity^{39–42}. The amount of adipose tissue that accumulates around the atria is associated with the risk, persistence, and severity of atrial fibrillation (AF). Antidiabetic drugs and lipid-lowering and surgical ablation of epicardial adipose tissue have been demonstrate to improve AF^{39,40}. Pericardial fat accumulation is also associated with alterations in heart rate variability⁴¹. Very long-chain acyl-CoA dehydrogenase catalyzes the first reaction of mitochondrial β -oxidation. A longer QTc interval

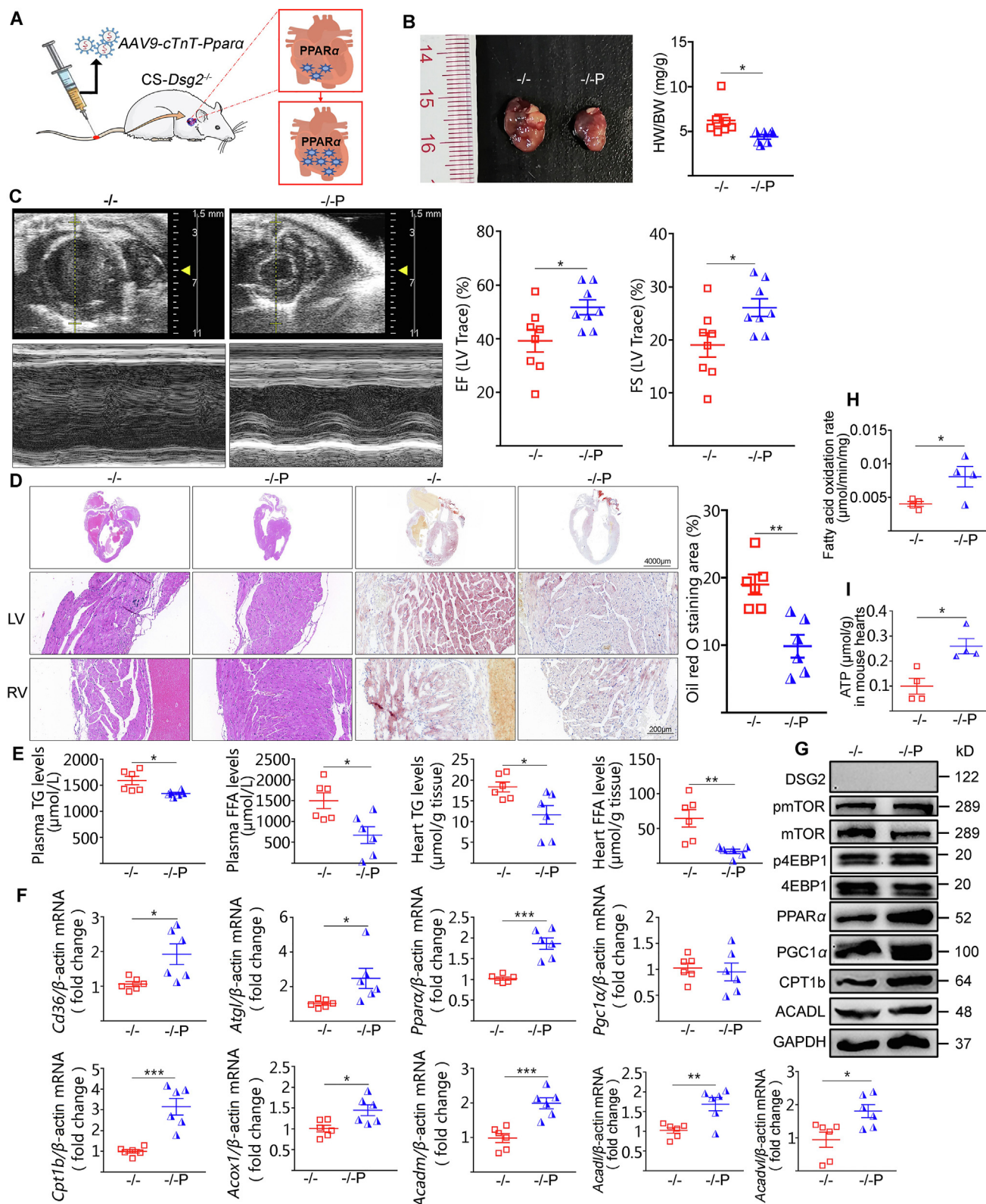


Figure 6 Reactivation of cardiac PPAR α by AAV9-Ppara improved cardiac dysfunction and lipid accumulation in CS-Dsg2^{-/-} mice. (A) Cardiac-specific PPAR α overexpression in mice. (B) Representative heart image, heart weight, body weight and heart/body weight ratio of WT, CS-Dsg2^{-/-} and CS-Dsg2^{-/-} mice treated with AAV9-Ppara (-/-P). (C) Representative echocardiographic images (M-Mode), EF and FS. (D) HE staining and Oil red O staining of heart sections. (E) Triglyceride and free fatty acid levels in plasma and heart. (F) Results of quantitative PCR analysis of *Cd36*, *Atgl*, *Ppara*, *Pgc1 α* , *Cpt1b*, *Acox1*, *Acadm*, *Acadl* and *Acadvl* mRNA levels in heart are expressed as fold change of control using β -actin as loading control. (G) Representative Western blots for DSG2, pmTOR, mTOR, p4EBP1, 4EBP1, PPAR α , PGC1 α , CPT1b, ACADL and GAPDH. Fatty acid oxidation rate (H) and ATP content (I) of heart. Results are expressed as mean values \pm SEM. $n = 5-8$. * $P < 0.05$, ** $P < 0.01$, *** $P < 0.001$ vs. CS-Dsg2^{-/-}.

and increased risk of sudden cardiac death were observed in very long-chain acyl-CoA dehydrogenase null mice⁴². Thus, impaired FA β -oxidation results in not only insufficient ATP production to support cardiac activity, but also lipid accumulation in cardiomyocytes, which explain the fatty deposition, arrhythmogenicity and HF seen in ACM patients.

Despite not referred to as “metabolic organ” generally, the heart is the organ that consumes the highest amount of energy in our body, which relies on highly sophisticated regulatory mechanisms to optimize energy use and protein turnover^{19,43}. mTOR is known as intracellular fuel sensor, which plays a crucial role in lipid homeostasis by controlling both anabolic and catabolic pathways⁴⁴. The anabolic processes of lipid metabolism include fatty acid synthesis, adipogenesis and esterification. The catabolic processes of lipid metabolism include hydrolysis of triglyceride to yield glycerol and FFA, followed by β -oxidation of FFA to yield acetyl CoA²⁶. mTORC1 has been shown to promote *de novo* lipogenesis in hepatocytes by activating the transcription factor, sterol regulatory element binding protein (SREBP), which in turn activates ACC⁴⁵, FAS⁴⁶, and SCD⁴⁷ enzymes involved in lipogenesis. S6K1 is found to mediate the upregulation of SREBP by mTORC1 in hepatocytes⁴⁷. The role of mTOR is extremely complicated in the heart. Doxycycline-induced cardiac-specific knockout of mTOR results in decreased FA β -oxidation and impaired cardiac function. mTOR-KO mice show marked dilation and fibrosis in heart and died in ten weeks after doxycycline induction⁴⁸. Similar results were found in cardiomyocyte-specific deletion of mTORC1 component raptor⁴⁹. Reduced FA oxidation but enhanced glucose oxidation was found in Raptor cKO mice, accompanied by downregulation of genes related to FA oxidation, such as PPAR α , PGC1 α and their downstream targets, which resulted in dilated cardiomyopathy with high mortality⁴⁹. These indicated an essential role of mTOR pathway in cardiac function by promoting FA oxidation. In contrast to the liver, 4EBP1, but not S6K1, is the critical mediator of mTOR in the heart^{26,50}. In concordance to these studies, we found decrement in mTOR–4EBP1–PPAR α signaling pathway results in impaired FA oxidation and cardiac function in the *Dsg2* deficient ACM mouse model. Inhibition of this pathway by rapamycin caused declined FA β -oxidation as well as deteriorated cardiac dysfunction, while overexpression of mTOR and 4EBP1 did the reverse. These findings suggested that the impaired FA β -oxidation in cardiac-specific *Dsg2* knockout mice was a result of defective mTOR–4EBP1–PPAR α signaling pathway, which deprived energy supply from FA β -oxidation and ultimately accelerated the development of cardiac dysfunction and lipid accumulation. Interestingly, although mTOR is vital to cardiac development and function from embryonic stage to adulthood, partial inhibition of mTOR exerts beneficial effects during aging and appear to increase cardiomyocyte resistance to aging stress⁵⁰. Moreover, mTOR is found to be activated in pressure-induced cardiac hypertrophy caused by transverse aortic constriction (TAC) or hypertension and rapamycin attenuates pressure-induced cardiac hypertrophy^{51–53}. mTOR is found to be inhibited during cardiomyocyte energy deprivation and ischemia⁵⁴, but activated during chronic myocardial infarction as a consequence of increased pressure load⁵⁵. Therefore, lines of evidences suggest that mTOR plays different roles in the heart in different circumstances and stages and use of rapamycin in cardiac dysfunction should be disease-dependent.

It should be noted that other metabolic pathway changes may also be involved in ACM. Kim et al.⁵⁶ generated an *in vitro* model

of ARVD/C using patient-derived induced pluripotent stem cell-derived cardiomyocytes, which displayed abnormal activation of PPAR γ and extensive lipogenesis in two ARVD/C patients with plakophilin-2 mutations. Song et al.⁵⁷ found elevated ketone metabolic enzymes in the RV of ACM patients with different genetic etiologies, suggesting higher ketone metabolism in ACM. Higher ketone metabolism was also validated in the patient-derived induced pluripotent stem cell-derived cardiomyocytes *in vitro*. Different alteration in metabolic pathways in ACM suggests heterogeneity in pathogenesis.

The most encouraging finding of our study was that reactivation of PPAR α , either by AAV-mediated overexpression or a PPAR α agonist fenofibrate, alleviated the lipid accumulation and improved the cardiac function in the *Dsg2* deletion-induced ACM. Currently, there is no curative or effective treatment for ACM. Treatments such as medication and lifestyle management are used to reduce and control symptoms, and reduce the risk of complications. Angiotensin converting enzyme inhibitors, angiotensin II receptor blockers, beta receptor inhibitors and anti-arrhythmic medication are commonly used for improving the pumping of heart, controlling arrhythmias and reducing the risk of complications⁵⁸. Fenofibrate is widely used in dyslipidemia treatment, which transcriptionally regulates the expression of critical genes in lipid and carbohydrate metabolism, leading to an increase in muscle β -oxidation and resulting in a reduction of plasma TG levels consequently^{59,60}. Fenofibrate effectively alleviates HF in the isoproterenol-induced rat model *via* promoting the FA oxidation⁶¹. In our present study, fenofibrate ameliorated cardiac dysfunction and lipid accumulation in CS-*Dsg2*^{-/-} mice through stimulating PPAR α -mediated FA β -oxidation. Meanwhile, targeting PPAR α activation by AAV9-*Ppara* also reversed *Dsg2* deletion-induced cardiac dysfunction and lipid accumulation. Our results suggests that PPAR α is a promising target for ACM treatment by alleviating the fatty deposition and improving cardiac function.

5. Conclusions

Our study generated an ACM model by cardiac-specific *Dsg2* knockout and suggested that impaired FA β -oxidation through inhibition of mTOR–4EBP1–PPAR α signaling pathway might underlie the pathogenesis of ACM ([Supporting Information Fig. S9](#)). Targeting PPAR α activation may be an effective means to combat excessive cardiac lipid deposition and impaired contractile function in ACM patients.

Acknowledgments

This work was supported by grants from the National Natural Science Foundation of China (82170818, 81770794, 31401001), the Fundamental Research Funds for the Central Universities (21620423, China), the Science and Technology Project of Zhuhai (20191210E030072, China).

Author contributions

Yubi Lin, Ruonan Liu and Geyang Xu designed the research. Yubi Lin, Ruonan Liu, Yanling Huang, Zhe Yang, Jianzhong Xian, Jingmin Huang, Zirui Qiu, Xiufang Lin, Mengzhen Zhang and Jiana Huang performed the experiments. Yubi Lin, Ruonan Liu, Jingmin Huang, Hui Chen, Huadong Wang and Geyang Xu

analyzed the data and edited the figures. Geyang Xu and Hui Chen wrote the manuscript. All authors contributed to the discussion and revised the article and all approved the final versions of the manuscript. Geyang Xu is responsible for the integrity of the work as a whole.

Conflicts of interest

The authors have no conflicts of interest to declare.

Appendix A. Supporting information

Supporting data to this article can be found online at <https://doi.org/10.1016/j.apsb.2022.05.018>.

References

- Corrado D, Link MS, Calkins H. Arrhythmogenic right ventricular cardiomyopathy. *N Engl J Med* 2017;**376**:61–72.
- Corrado D, Basso C, Pavei A, Michieli P, Schiavon M, Thiene G. Trends in sudden cardiovascular death in young competitive athletes after implementation of a preparticipation screening program. *JAMA* 2006;**296**:1593–601.
- Corrado D, Wichter T, Link MS, Hauer R, Marchlinski F, Anastasakis A, et al. Treatment of arrhythmogenic right ventricular cardiomyopathy/dysplasia: an international task force consensus statement. *Eur Heart J* 2015;**36**:3227–37.
- Maron BJ, Towbin JA, Thiene G, Antzelevitch C, Corrado D, Arnett D, et al. Contemporary definitions and classification of the cardiomyopathies: an american heart association scientific statement from the council on clinical cardiology, heart failure and transplantation committee; quality of care and outcomes research and functional genomics and translational biology interdisciplinary working groups; and council on epidemiology and prevention. *Circulation* 2006;**113**:1807–16.
- Pilichou K, Nava A, Basso C, Beffagna G, Bauce B, Lorenzon A, et al. Mutations in desmoglein-2 gene are associated with arrhythmogenic right ventricular cardiomyopathy. *Circulation* 2006;**113**:1171–9.
- Syrris P, Ward D, Evans A, Asimaki A, Gandjbakhch E, Sen-Chowdhry S, et al. Arrhythmogenic right ventricular dysplasia/cardiomyopathy associated with mutations in the desmosomal gene desmocollin-2. *Am J Hum Genet* 2006;**79**:978–84.
- McKoy G, Protonotarios N, Crosby A, Tsatsopoulou A, Anastasakis A, Coonar A, et al. Identification of a deletion in plakoglobin in arrhythmogenic right ventricular cardiomyopathy with palmoplantar keratoderma and woolly hair (Naxos disease). *Lancet* 2000;**355**:2119–24.
- Alcalai R, Metzger S, Rosenheck S, Meiner V, Chajek-Shaul T. A recessive mutation in desmoplakin causes arrhythmogenic right ventricular dysplasia, skin disorder, and woolly hair. *J Am Coll Cardiol* 2003;**42**:319–27.
- Gerull B, Heuser A, Wichter T, Paul M, Basson CT, McDermott DA, et al. Mutations in the desmosomal protein plakophilin-2 are common in arrhythmogenic right ventricular cardiomyopathy. *Nat Genet* 2004;**36**:1162–4.
- Al-Amoudi A, Diez DC, Betts MJ, Frangakis AS. The molecular architecture of cadherins in native epidermal desmosomes. *Nature* 2007;**450**:832–7.
- Tariq H, Bella J, Jowitt TA, Holmes DF, Rouhi M, Nie Z, et al. Cadherin flexibility provides a key difference between desmosomes and adherens junctions. *Proc Natl Acad Sci U S A* 2015;**112**:5395–400.
- Dieding M, Debus JD, Kerkhoff R, Gaertner-Rommel A, Walhorn V, Miltung H, et al. Arrhythmogenic cardiomyopathy related DSG2 mutations affect desmosomal cadherin binding kinetics. *Sci Rep* 2017;**7**:13791.
- Harrison OJ, Brasch J, Lasso G, Katsamba PS, Ahlsen G, Honig B, et al. Structural basis of adhesive binding by desmocollins and desmogleins. *Proc Natl Acad Sci U S A* 2016;**113**:7160–5.
- Hermida A, Fressart V, Hidden-Lucet F, Donal E, Probst V, Deharo JC, et al. High risk of heart failure associated with desmoglein-2 mutations compared to plakophilin-2 mutations in arrhythmogenic right ventricular cardiomyopathy/dysplasia. *Eur J Heart Fail* 2019;**21**:792–800.
- Pilichou K, Remme CA, Basso C, Campian ME, Rizzo S, Barnett P, et al. Myocyte necrosis underlies progressive myocardial dystrophy in mouse *dsg2*-related arrhythmogenic right ventricular cardiomyopathy. *J Exp Med* 2009;**206**:1787–802.
- Kant S, Krull P, Eisner S, Leube RE, Krusche CA. Histological and ultrastructural abnormalities in murine desmoglein 2-mutant hearts. *Cell Tissue Res* 2012;**348**:249–59.
- Volani C, Rainer J, Hernandez VV, Meraviglia V, Pramstaller PP, Smárason SV, et al. Metabolic signature of arrhythmogenic cardiomyopathy. *Metabolites* 2021;**11**:195.
- Bertero E, Maack C. Metabolic remodelling in heart failure. *Nat Rev Cardiol* 2018;**15**:457–70.
- Stanley WC, Recchia FA, Lopaschuk GD. Myocardial substrate metabolism in the normal and failing heart. *Physiol Rev* 2005;**85**:1093–129.
- Heather LC, Cole MA, Lygate CA, Evans RD, Stuckey DJ, Murray AJ, et al. Fatty acid transporter levels and palmitate oxidation rate correlate with ejection fraction in the infarcted rat heart. *Cardiovasc Res* 2006;**72**:430–7.
- Osorio JC, Stanley WC, Linke A, Castellari M, Diep QN, Panchal AR, et al. Impaired myocardial fatty acid oxidation and reduced protein expression of retinoid X receptor- α in pacing-induced heart failure. *Circulation* 2002;**106**:606–12.
- Dávila-Román VG, Vedala G, Herrero P, de las Fuentes L, Rogers JG, Kelly DP, et al. Altered myocardial fatty acid and glucose metabolism in idiopathic dilated cardiomyopathy. *J Am Coll Cardiol* 2002;**40**:271–7.
- Bedi Jr KC, Snyder NW, Brandimarto J, Aziz M, Mesaros C, Worth AJ, et al. Evidence for intramyocardial disruption of lipid metabolism and increased myocardial ketone utilization in advanced human heart failure. *Circulation* 2016;**133**:706–16.
- Kaimoto S, Hoshino A, Ariyoshi M, Okawa Y, Tateishi S, Ono K, et al. Activation of PPAR- α in the early stage of heart failure maintained myocardial function and energetics in pressure-overload heart failure. *Am J Physiol Heart Circ Physiol* 2017;**312**:H305–13.
- Haemmerle G, Moustafa T, Woelkart G, Büttner S, Schmidt A, van de Weijer T, et al. ATGL-mediated fat catabolism regulates cardiac mitochondrial function via PPAR- α and PGC-1. *Nat Med* 2011;**17**:1076–85.
- Xu L, Brink M. mTOR, cardiomyocytes and inflammation in cardiac hypertrophy. *Biochim Biophys Acta* 2016;**1863**:1894–903.
- Sciarretta S, Forte M, Frati G, Sadoshima J. New insights into the role of mTOR signaling in the cardiovascular system. *Circ Res* 2018;**122**:489–505.
- Zhu Y, Pires KM, Whitehead KJ, Olsen CD, Wayment B, Zhang YC, et al. Mechanistic target of rapamycin (*Mtor*) is essential for murine embryonic heart development and growth. *PLoS One* 2013;**8**:e54221.
- Tsai S, Sitzmann JM, Dastidar SG, Rodriguez AA, Vu SL, McDonald CE, et al. Muscle-specific 4E-BP1 signaling activation improves metabolic parameters during aging and obesity. *J Clin Invest* 2015;**125**:2952–64.
- Chen Q, Chen L, Jian J, Li J, Zhang X. The mechanism behind BAF60c in myocardial metabolism in rats with heart failure is through the PGC1 α -PPAR α -mTOR signaling pathway. *Biochem Cell Biol* 2020:1–11.
- Xu G, Li Z, Ding L, Tang H, Guo S, Liang H, et al. Intestinal mTOR regulates GLP-1 production in mouse L cells. *Diabetologia* 2015;**58**:1887–97.
- Jin B, Shi H, Zhu J, Wu B, Geshang Q. Up-regulating autophagy by targeting the mTOR-4EBP1 pathway: a possible mechanism for improving cardiac function in mice with experimental dilated cardiomyopathy. *BMC Cardiovasc Disord* 2020;**20**:56.

33. Thiene G, Nava A, Corrado D, Rossi L, Pennelli N. Right ventricular cardiomyopathy and sudden death in young people. *N Engl J Med* 1988;**318**:129–33.
34. Marcus FI, Fontaine GH, Guiraudon G, Frank R, Laurenceau JL, Malergue C, et al. Right ventricular dysplasia: a report of 24 adult cases. *Circulation* 1982;**65**:384–98.
35. Chen L, Rao M, Chen X, Chen K, Ren J, Zhang N, et al. A founder homozygous *DSG2* variant in East Asia results in ARVC with full penetrance and heart failure phenotype. *Int J Cardiol* 2019;**274**:263–70.
36. Bhonsale A, Groeneweg JA, James CA, Dooijes D, Tichnell C, Jongbloed JD, et al. Impact of genotype on clinical course in arrhythmogenic right ventricular dysplasia/cardiomyopathy-associated mutation carriers. *Eur Heart J* 2015;**36**:847–55.
37. Lin Y, Huang J, Zhao T, He S, Huang Z, Chen X, et al. Compound and heterozygous mutations of *DSG2* identified by whole exome sequencing in arrhythmogenic right ventricular cardiomyopathy/dysplasia with ventricular tachycardia. *J Electrocardiol* 2018;**51**:837–43.
38. Eshkind L, Tian Q, Schmidt A, Franke WW, Windoffer R, Leube RE. Loss of desmoglein 2 suggests essential functions for early embryonic development and proliferation of embryonal stem cells. *Eur J Cell Biol* 2002;**81**:592–8.
39. Hatem SN, Redheuil A, Gandjbakhch E. Cardiac adipose tissue and atrial fibrillation: the perils of adiposity. *Cardiovasc Res* 2016;**109**:502–9.
40. Zhou M, Wang H, Chen J, Zhao L. Epicardial adipose tissue and atrial fibrillation: possible mechanisms, potential therapies, and future directions. *Pacing Clin Electrophysiol* 2020;**43**:133–45.
41. Uceda DE, Zhu XY, Woollard JR, Ferguson CM, Patras I, Carlson DF, et al. Accumulation of pericardial fat is associated with alterations in heart rate variability patterns in hypercholesterolemic pigs. *Circ Arrhythm Electrophysiol* 2020;**13**:e007614.
42. Gélinas R, Thompson-Legault J, Bouchard B, Daneault C, Mansour A, Gillis MA, et al. Prolonged QT interval and lipid alterations beyond β -oxidation in very long-chain acyl-CoA dehydrogenase null mouse hearts. *Am J Physiol Heart Circ Physiol* 2011;**301**:H813–23.
43. Carley AN, Taegtmeier H, Lewandowski ED. Matrix revisited: mechanisms linking energy substrate metabolism to the function of the heart. *Circ Res* 2014;**114**:717–29.
44. Laplante M, Sabatini DM. mTOR signaling in growth control and disease. *Cell* 2012;**149**:274–93.
45. Brown NF, Stefanovic-Racic M, Sipula IJ, Perdomo G. The mammalian target of rapamycin regulates lipid metabolism in primary cultures of rat hepatocytes. *Metabolism* 2007;**56**:1500–7.
46. Peng T, Golub TR, Sabatini DM. The immunosuppressant rapamycin mimics a starvation-like signal distinct from amino acid and glucose deprivation. *Mol Cell Biol* 2002;**22**:5575–84.
47. Mauvoisin D, Rocque G, Arfa O, Radenne A, Boissier P, Mounier C. Role of the PI3-kinase/mTOR pathway in the regulation of the stearoyl CoA desaturase (*SCD1*) gene expression by insulin in liver. *J Cell Commun Signal* 2007;**1**:113–25.
48. Düvel K, Yecies JL, Menon S, Raman P, Lipovsky AI, Souza AL, et al. Activation of a metabolic gene regulatory network downstream of mTOR complex 1. *Mol Cell* 2010;**39**:171–83.
49. Shende P, Plaisance I, Morandi C, Pelliex C, Berthonneche C, Zorzato F, et al. Cardiac raptor ablation impairs adaptive hypertrophy, alters metabolic gene expression, and causes heart failure in mice. *Circulation* 2011;**123**:1073–82.
50. Sciarretta S, Volpe M, Sadoshima J. Mammalian target of rapamycin signaling in cardiac physiology and disease. *Circ Res* 2014;**114**:549–64.
51. Shioi T, McMullen JR, Tarnavski O, Converso K, Sherwood MC, Manning WJ, et al. Rapamycin attenuates load-induced cardiac hypertrophy in mice. *Circulation* 2003;**107**:1664–70.
52. McMullen JR, Sherwood MC, Tarnavski O, Zhang L, Dorfman AL, Shioi T, et al. Inhibition of mTOR signaling with rapamycin regresses established cardiac hypertrophy induced by pressure overload. *Circulation* 2004;**109**:3050–5.
53. Sciarretta S, Zhai P, Shao D, Maejima Y, Robbins J, Volpe M, et al. Rheb is a critical regulator of autophagy during myocardial ischemia: pathophysiological implications in obesity and metabolic syndrome. *Circulation* 2012;**125**:1134–46.
54. Buss SJ, Muenz S, Riffel JH, Malekar P, Hagenmueller M, Weiss CS, et al. Beneficial effects of mammalian target of rapamycin inhibition on left ventricular remodeling after myocardial infarction. *J Am Coll Cardiol* 2009;**54**:2435–46.
55. Völkers M, Konstandin MH, Doroudgar S, Toko H, Quijada P, Din S, et al. Mechanistic target of rapamycin complex 2 protects the heart from ischemic damage. *Circulation* 2013;**128**:2132–44.
56. Kim C, Wong J, Wen J, Wang S, Wang C, Spiering S, et al. Studying arrhythmogenic right ventricular dysplasia with patient-specific iPSCs. *Nature* 2013;**494**:105–10.
57. Song JP, Chen L, Chen X, Ren J, Zhang NN, Tirasawasdichai T, et al. Elevated plasma beta-hydroxybutyrate predicts adverse outcomes and disease progression in patients with arrhythmogenic cardiomyopathy. *Sci Transl Med* 2020;**12**:2132–44.
58. Towbin JA, McKenna WJ, Abrams DJ, Ackerman MJ, Calkins H, Darrioux FCC, et al. 2019 HRS expert consensus statement on evaluation, risk stratification, and management of arrhythmogenic cardiomyopathy: executive summary. *Heart Rhythm* 2019;**16**:e373–407.
59. Balakumar P, Sambathkumar R, Mahadevan N, Muhsinah AB, Alsayari A, Venkateswaramurthy N, et al. Molecular targets of fenofibrate in the cardiovascular-renal axis: a unifying perspective of its pleiotropic benefits. *Pharmacol Res* 2019;**144**:132–41.
60. Pettersen JC, Pruimboom-Brees I, Francone OL, Amacher DE, Boldt SE, Kerlin RL, et al. The PPAR α agonists fenofibrate and CP-778875 cause increased beta-oxidation, leading to oxidative injury in skeletal and cardiac muscle in the rat. *Toxicol Pathol* 2012;**40**:435–47.
61. Li P, Luo S, Pan C, Cheng X. Modulation of fatty acid metabolism is involved in the alleviation of isoproterenol-induced rat heart failure by fenofibrate. *Mol Med Rep* 2015;**12**:7899–906.